



Cite this: *Chem. Commun.*, 2014, 50, 13454

Received 15th July 2014,  
Accepted 9th September 2014

DOI: 10.1039/c4cc05439c

[www.rsc.org/chemcomm](http://www.rsc.org/chemcomm)

**The synthesis of new conjugated building blocks, diselenolodiselenole ( $C_4Se_4$ ) derivatives, is described for the first time. The structural and optoelectronic properties of  $C_4Se_4$ -derivatives are tuned by varying end-capping aromatic substituents. In cyclic voltammetry, all  $C_4Se_4$ -derivatives show two reversible oxidation peaks.**

Organoselenium compounds have attracted considerable interest due to their wide range of applications in many fields.<sup>1</sup> Chalcogenophene containing building blocks are being given great importance to synthesize new conjugated organic materials. Their applications in the state-of-the-art technologies including field-effect transistors, flexible light emitting diodes and organic photovoltaics are being extensively studied.<sup>2</sup> Though the development in this field has grown rapidly in the last two decades, the conjugated electroactive building blocks with promising properties are limited.<sup>3</sup> Conjugated chalcogenophene based materials with reversible redox activity have found applications in organic electronic devices.<sup>4</sup>

Though the applications of thiophene based electroactive small molecules or polymers in organic electronics have attracted considerable research attention, their selenium counterparts are sparsely reported.<sup>5–7</sup> Partly, it can be ascribed to the difficulties in the synthesis of selenophene derivatives and their instabilities in the charged states. The advantages of replacement of sulfur by selenium in conjugated systems are manifold: (a) intermolecular  $Se \cdots Se$  interactions lead to a wide bandwidth in organic conductors, which should facilitate intermolecular charge transfer, (b) selenium containing organoheterooles have lower oxidation and reduction potentials than that of sulfur containing heterocycles, (c) due to higher polarizability of Se than that of S, compounds with the selenium atom attached to the conjugated

backbone possess more polarizability than their sulfur analogues, (d) selenium containing compounds should have a lower band gap than their sulfur counterparts and, consequently, their optoelectronic properties also differ.

Blum and co-workers reported the synthesis of the first example of dithiolodithiole ( $C_4S_4$ ) derivatives in 26% yield from 1,4-diphenylbutadiyne and elemental sulfur at 150 °C for 52 h.<sup>8</sup> The growing interest in the  $C_4S_4$  systems led to the development of a more facile synthetic strategy and a systematic study reported by Swager *et al* focusing on their interesting structural and optoelectronic properties.<sup>9</sup> According to Hückel's rule, the  $C_4S_4$  system is formally anti-aromatic in the ground state and non-aromatic in the excited state; thus these molecules can lead to interesting electronic properties. The structural and electronic properties of these systems can be further tuned by an atomistic approach by replacing S with Se, which may lead to a more interesting and important fused conjugated system ( $C_4Se_4$ ). Here, we present for the first time the synthesis of diselenolodiselenole ( $C_4Se_4$ ) derivatives, bicyclic heterocycles, as a new class of conjugated building blocks.

We have synthesized a series of compounds containing  $C_4Se_4$  as the central conjugated system. The precursor diyne compounds **1a**,<sup>10</sup> **1c**<sup>11</sup> and **1e**<sup>12</sup> were prepared by a previously reported procedure. Dynes **1b** and **1d** were synthesized by new synthetic methods (see ESI†). The conversion of dynes to  $C_4Se_4$  derivatives could proceed through the radical mechanism similar to the formation of  $C_4S_4$  derivatives.<sup>9</sup> However, the reaction of **1a** with Se powder in the presence of solvent (1,2-dichloroethane (DCE)-*o*-dichlorobenzene (*o*-DCB)) and the radical initiator (azobisisobutyronitrile (AIBN)-2,2,6,6-tetramethylpiperidinyloxy (TEMPO)) at 190 °C in a pressure vessel with and without microwaves resulted in very low yields (Scheme 1, conditions I and II).

Moreover, heating of elemental selenium with **1a** nearly at the melting point of selenium without any solvents afforded the best yield of 23% for **2a** (Scheme 1, condition III). Therefore, condition III was considered as a general procedure to prepare  $C_4Se_4$  derivatives **2a–2e** from diyne precursors (Scheme 2). The yields were obtained in the range of 10–30%. Though the strongly electron donating substituents on the phenyl ring were reasoned to cause a

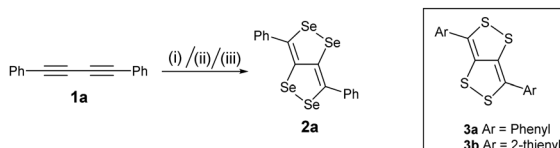
Department of Chemical Sciences, Indian Institute of Science Education and Research (IISER) Kolkata, Mohanpur 714246, India.

E-mail: [sanjiozade@iiserkol.ac.in](mailto:sanjiozade@iiserkol.ac.in)

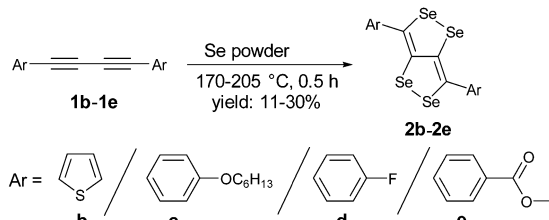
† Dedicated to the memory of Professor Michael Bendikov.

‡ Electronic supplementary information (ESI) available: Details of experimental procedures, characterization, and the crystallographic parameter table. CCDC 1011954, 1011956 and 1011963. For ESI and crystallographic data in CIF or other electronic format see DOI: 10.1039/c4cc05439c





**Scheme 1** Synthesis of **2a**. (i) Se powder, AIBN in the pressure vessel with DCE at 190 °C for 48 h, yield = 2%. (ii) Se powder, TEMPO with *o*-dichlorobenzene at 190 °C in microwave for 1 h, yield = 2%. (iii) Se powder in the Schlenk flask at 190 °C for 0.5 h, yield = 23%.



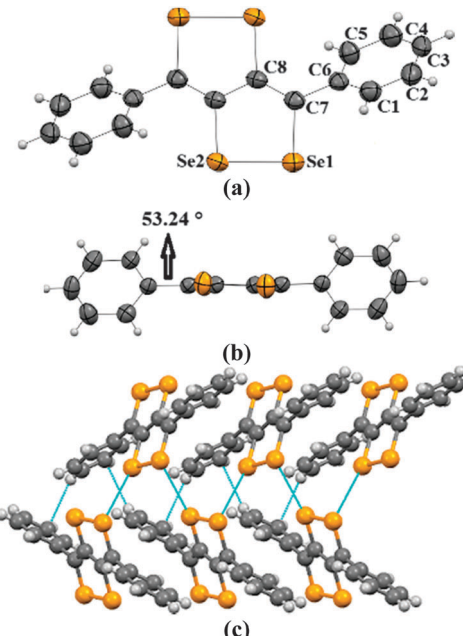
**Scheme 2** Synthesis of  $\text{C}_4\text{Se}_4$  derivatives **2b-2e**.

complex mixture of the product and low yield in the case of  $\text{C}_4\text{S}_4$  derivatives,<sup>9</sup> the reaction of di(*p*-hexyloxyphenyl) diacetylene (**1c**) afforded the highest yield (30%) in this series.

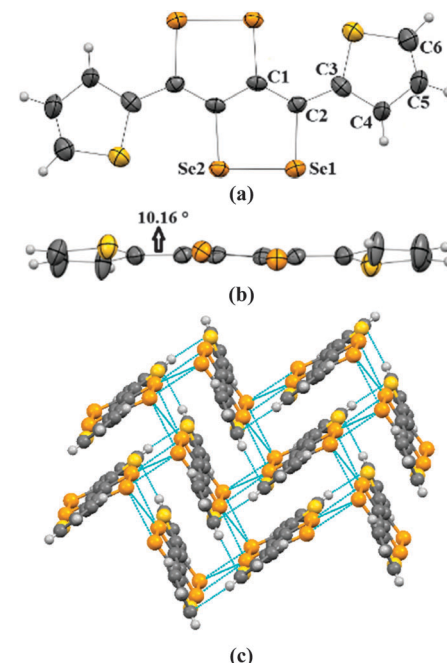
Crystals of **2a-2c** were obtained by the slow evaporation method from their solution in dichloromethane (DCM). In the crystal structure of **2a**, capped phenyl rings are twisted from the  $\text{C}_4\text{Se}_4$  core by a dihedral angle of  $\sim 53^\circ$  ( $\text{C}8-\text{C}7-\text{C}6-\text{C}5 = 126.8(4)$ ) (Fig. 1a and b), which is significantly higher (by  $\sim 28^\circ$ ) than that of sulfur analogue **3a**.<sup>9</sup> Molecules of **2a** form end-to-end dimers *via* intermolecular  $\pi-\pi$  interactions ( $\text{C}4-\text{C}5 = 3.91 \text{ \AA}$  and  $\text{C}4-\text{C}4 = 3.37 \text{ \AA}$ ). Selenium atoms of the Se-Se bond of **2a** form  $\text{Se}\cdots\text{Se}$  interactions ( $\text{Se}1\cdots\text{Se}2 = 3.64 \text{ \AA}$ ) with the neighboring two molecules. This leads to the formation of a virtual  $(\text{Se}-\text{Se}\cdots\text{Se}-\text{Se})_n$  polymeric chain along the *c*-axis, from which the phenyl rings are hanged like pendants (Fig. 1c), whereas in the crystal packing of **3a**, face-to-face dimer formation was observed *via*  $\text{S}\cdots\text{S}$  interactions.<sup>9</sup> Interestingly, in the case of thiophene capped  $\text{C}_4\text{Se}_4$  (**2b**) the torsional angle between the outer thiophene ring and the central  $\text{C}_4\text{Se}_4$  unit is found to be only  $\sim 10^\circ$  ( $\text{C}1-\text{C}2-\text{C}3-\text{C}4 = 169.3(7)$ ) (Fig. 2a and b). The nearly planar conjugated backbone of **2b** exhibited resolute intermolecular interactions through heteroatoms.

In the crystal structure of **2b**, a pair of Se atoms of each diselenole unit forms two perpendicular dimers by three different  $\text{Se}\cdots\text{Se}$  interactions ( $\text{Se}1\cdots\text{Se}1 = 3.648(1)$  and  $\text{Se}2\cdots\text{Se}1 = 3.525(1)$ ,  $\text{Se}2\cdots\text{Se}2 = 3.726(1)$ ) with the diselenole unit of neighboring molecules (Fig. 2c). Thus four molecules connected by  $\text{Se}\cdots\text{Se}$  and  $\pi\cdots\text{H}-\text{C}$  interactions ( $\text{C}6-\text{H}6 = 2.81 \text{ \AA}$ ) form a 2D brick-like structure in bulk. This 2D crystal packing with several nonbonding interactions could facilitate the intermolecular charge transport. In **2c** the dihedral angle between the hexyloxy substituted phenyl ring and the central  $\text{C}_4\text{Se}_4$  unit is  $\sim 58^\circ$  ( $\text{C}8-\text{C}3-\text{C}2-\text{C}1 = -122.4(5)$ ) (Fig. S1, ESI<sup>‡</sup>).

DFT optimized structures (at B3LYP/6-31G(d)) of **2a** and **2b** showed dihedral angles of  $47^\circ$  and  $0^\circ$ , respectively, between the central  $\text{C}_4\text{Se}_4$  unit and end-capping substituents. Corresponding values for  $\text{C}_4\text{S}_4$  derivatives are  $39^\circ$  and  $0^\circ$ , respectively.



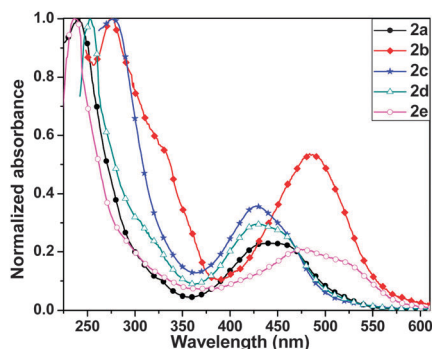
**Fig. 1** (a) ORTEP diagram of **2a**, (b) torsional angle in **2a**, and (c) packing of **2a**. The ellipsoids are drawn at the 50% probability level in (a) and (b).



**Fig. 2** (a) ORTEP diagram of **2b**, (b) torsional angle in **2b**, and (c) packing of **2b**. The ellipsoids are drawn at the 50% probability level in (a) and (b).

Compounds **2a-2e** exhibited two sets of absorption peaks with  $\lambda_{\text{max}}$  ranging from 236 to 277 nm and 427 to 484 nm, respectively (Fig. 3 and Table 1). Compound **2a** showed  $\lambda_{\text{max}}$  at 440 nm in solution, which was blue shifted compared to its  $\text{C}_4\text{S}_4$  analogues. This may be ascribed to the large dihedral angle between the outer phenyl rings and the central  $\text{C}_4\text{Se}_4$  unit that reduces the effective overlap between these two conjugated



Fig. 3 UV-vis spectra of **2a**–**2e** in DCM.Table 1 Yields, absorption and electrochemical properties of **2a**–**2e**

| Compound  | Yield (%) | $\lambda_{\max}$ (nm) | $E_{1/2}$ vs. Ag/Ag <sup>+</sup> (V) | $E_g^{\text{opt}}\text{a}$ (eV) | HOMO <sup>b</sup> (eV) | LUMO <sup>c</sup> (eV) |
|-----------|-----------|-----------------------|--------------------------------------|---------------------------------|------------------------|------------------------|
| <b>2a</b> | 23        | 240, 440              | 0.35, 0.86                           | 2.39                            | -4.79                  | -2.40                  |
| <b>2b</b> | 12        | 275, 484              | 0.47, 0.98                           | 2.21                            | -4.91                  | -2.70                  |
| <b>2c</b> | 30        | 277, 428              | 0.25, 0.77                           | 2.46                            | -4.69                  | -2.23                  |
| <b>2d</b> | 15        | 253, 427              | 0.49, 1.03                           | 2.43                            | -4.93                  | -2.50                  |
| <b>2e</b> | 19        | 236, 475              | 0.50, 1.04                           | 2.15                            | -4.94                  | -2.79                  |

<sup>a</sup>  $E_g^{\text{opt}} = 1240/\lambda_{\text{onset}}$ . <sup>b</sup>  $E_{\text{HOMO}} = -(4.44 + E_{1/2})$ . <sup>c</sup>  $E_{\text{LUMO}} = E_{\text{HOMO}} + E_g^{\text{opt}}$ .

parts. A similar trend was observed in the absorption spectra of **2c** and **2d**. The absorption spectrum of **2e** was red shifted compared to that of **2a**, **2c** and **2d**.  $E_g^{\text{opt}}$  of **2e** is very close to its corresponding  $\text{C}_4\text{S}_4$  analogue. It may be considered as a counterbalance of the blue shift in the absorption of **2e** due to a larger dihedral angle than that of  $\text{C}_4\text{S}_4$  by the red shift due to better electron donating properties of  $\text{C}_4\text{Se}_4$  than that of  $\text{C}_4\text{S}_4$  in the presence of the stronger electron accepting carboxylate substituted capped phenyl rings. The highest value of  $\lambda_{\max}$  for **2b** among all  $\text{C}_4\text{Se}_4$  derivatives is due to its nearly planar structures, which allow the effective end-to-end conjugation and enhance donor–acceptor properties.

All  $\text{C}_4\text{Se}_4$  derivatives **2a**–**2e** exhibited two reversible oxidation potentials in the range of 0.30–0.54 V and 0.90–1.10 V, respectively, in cyclic voltammetry (CV) experiments (Fig. 4) similar to that of  $\text{C}_4\text{S}_4$  derivatives.<sup>9</sup> The variation in the oxidation potentials of **2a** and **2c**–**2e** could be understood on the basis of substituents on capped phenyl rings. Though thiophene is electron rich compared

to benzene, **2b** has higher oxidation potentials than those of **2a**, and it is comparable with those of **2d** and **2e**. The planar structure of **2b** could result in improved delocalization of the electrons of the  $\text{C}_4\text{Se}_4$  unit throughout the conjugated backbone, which could decrease the electron density on the  $\text{C}_4\text{Se}_4$  unit. The planarity of the conjugated core in **2b** assisted the selenium atoms to exert the effect of its larger polarizability and less electronegativity on the extended conjugation. The first oxidation potential of  $\text{C}_4\text{Se}_4$  derivatives is nearly in the same range as that of  $\text{C}_4\text{S}_4$  derivatives, however, the difference between the first and second oxidation potentials is  $\sim 0.1$  V less than that of  $\text{C}_4\text{S}_4$  derivatives.<sup>9</sup>

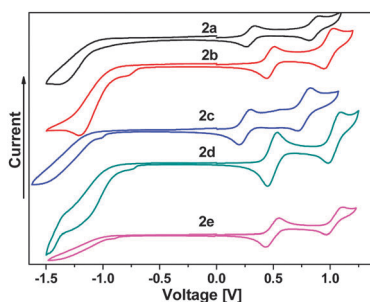
Discussion of DFT calculated absorption spectra, HOMO–LUMO energy values, HOMO–LUMO gaps of **2a** and **2b** and comparison with  $\text{C}_4\text{S}_4$  derivatives and experimental results is given in ESI‡ (Table S2, Fig. S2 and S3).

In summary, a new class of conjugated compounds, diselenolodiselenoles, was successfully synthesized simply by heating diaryl diynes with elemental selenium. The structural and optoelectronic properties of diselenolodiselenole derivatives can be tuned by the judicious choice of the capped aryl groups. The thiophene capped  $\text{C}_4\text{Se}_4$  displayed a nearly planar structure with its absorption at the highest wavelength among the compounds in the present series. Therefore, it is a promising candidate to be exploited for application in organic electronics. Due to the presence of Se–Se interactions, diselenolodiselenole derivatives can arrange into interesting crystalline motifs. Thus, we have shown that the structural engineering and atomistic approach could be beneficial to synthesize meaningful building blocks for conjugated systems.

This work is supported by CSIR, India.

## Notes and references

- (a) *Chemistry of Organic Selenium and Tellurium Compounds*, ed. Z. Rappoport, Wiley, Chichester, 2012, vol. 3, 2014, 4; (b) A. J. Mukherjee, S. S. Zade, H. B. Singh and R. B. Sunoj, *Chem. Rev.*, 2010, **110**, 4357.
- (a) *Handbook of Organic Conductive Molecules and Polymers*, ed. H. S. Nalwa, John Wiley & Sons, New York, 1997, vol. 1–4; (b) A. Facchetti, *Chem. Mater.*, 2011, **23**, 733.
- Handbook of Thiophene-based Materials: Applications in Organic Electronics and Photonics*, ed. I. F. Perekopchka and D. F. Perekopchka, John Wiley & Sons, New York, 2009, vol. 1 and 2.
- (a) P. M. Beaujuge and J. R. Reynolds, *Chem. Rev.*, 2010, **110**, 268; (b) C. M. Amb, A. L. Dyer and J. R. Reynolds, *Chem. Mater.*, 2011, **23**, 397.
- (a) A. Patra and M. Bendikov, *J. Mater. Chem.*, 2010, **20**, 422; (b) A. Patra, R. Kumar and S. Chand, *Isr. J. Chem.*, 2014, **54**, 621; (c) J. Hollinger, D. Gao and D. S. Seferos, *Isr. J. Chem.*, 2014, **54**, 440.
- (a) S. Das and S. S. Zade, *Chem. Commun.*, 2010, **46**, 1168; (b) S. Das, A. Bedi, G. Rama Krishna, C. M. Reddy and S. S. Zade, *Org. Biomol. Chem.*, 2011, **9**, 6963; (c) A. Bedi, S. P. Senanayak, K. S. Narayan and S. S. Zade, *Macromolecules*, 2013, **46**, 5943.
- A. Patra, Y. H. Wijsboom, S. S. Zade, M. Li, Y. Sheynin, G. Leitus and M. Bendikov, *J. Am. Chem. Soc.*, 2008, **130**, 6734.
- J. Blum, Y. Badrieh, O. Shaaya, L. Meltser and H. Schumann, *Phosphorus, Sulfur Silicon Relat. Elem.*, 1993, **79**, 87.
- D. J. Schipper, L. C. H. Moh, P. Müller and T. M. Swager, *Angew. Chem., Int. Ed.*, 2014, **53**, 5847.
- I. D. Campbell and G. Eglinton, *Org. Synth.*, 1965, **45**, 39.
- Y. Arakawa, S. Nakajima, R. Ishige, M. Uchimura, S. Kang, G.-i. Konishi and J. Watanabe, *J. Mater. Chem.*, 2012, **22**, 8394.
- G. Zhang, H. Yi, G. Zhang, Y. Deng, R. Bai, H. Zhang, J. T. Miller, A. J. Kropf, E. E. Bunel and A. Lei, *J. Am. Chem. Soc.*, 2014, **136**, 924.

Fig. 4 Electrochemical properties of compounds **2a**–**2e** in 0.1 M TBAPF<sub>6</sub> in dry DCM as solvent using a Pt-disk working electrode, a Pt-wire counter electrode and a Ag/AgCl reference electrode.